ORIGINAL RESEARCH PAPER

Coexisting arsenate and arsenite adsorption from water using porous pellet adsorbent: Optimization by response surface methodology

B. Te*, B. Wichitsathian, C. Yossapol, W. Wonglertarak

School of Environmental Engineering, Institute of Engineering, Suranaree University of Technology, Nakhon Ratchasima 30000, Thailand

ABSTRACT: Mesoporous pellet adsorbent developed from mixing at an appropriate ratio of natural clay, iron oxide, iron powder, and rice bran was used to investigate the optimization process of batch adsorption parameters for treating aqueous solution coexisting with arsenate and arsenite. Central composite design under response surface methodology was applied for optimizing and observing both individual and interactive effects of four main influential adsorption factors such as contact time (24-72 h), initial solution pH (3-11), adsorbent dosage (0-20 g/L) and initial adsorbate concentration (0.25-4.25 mg/L). Analysis of variance suggested that experimental data were better fitted by the quadratic model with the values of regression coefficient and adjusted regression coefficient higher than 95%. The model accuracy was supported by the correlation plot of actual and predicted adsorption efficiency data and the residual plots. The Pareto analysis suggested that initial solution pH, initial adsorbate concentration, and adsorbent dosage had greater cumulative effects on the removal system by contributing the percentage effect of 47.69%, 37.07% and 14.26%, respectively. The optimum values of contact time, initial solution pH, adsorbent dosage and initial adsorbate concentration were 52 h, 7, 10 g/L and 0.5 mg/L, respectively. The adsorption efficiency of coexisting arsenate and arsenite solution onto the new developed adsorbent was over 99% under the optimized experimental condition.

KEYWORDS: *Analysis of variance; Arsenic removal; Central composite design; Mesoporous adsorbent; Response surface methodology.*

INTRODUCTION

Arsenic is a global well-known problematic contaminant and considered as a highly toxic and carcinogenic element by some international agencies such as International Agency for Research on Cancer (IARC) and the United State Environmental Protection Agency (USEPA) (Bhatia, *et al.*, 2014). Natural processes (weathering reactions, biological activities and volcanic emissions) and human activities (mining activities, consumption of fossil fuels and use of arsenic-containing pesticides or herbicides) are the main sources of presenting arsenic and its mobility in the environmental media (Villaescusa and Bollinger, 2008). In natural water, As concentration can be found up to 5000 µg/L, which is much higher than the maximum recommended level (10 µg/L) set by the World Health Organization (WHO) for drinking water (Habuda-Stanic and Nujic, 2015). As concentration (> 10 µg/L) in groundwater has been reported in 105 countries and put a risk of health hazard to over 200 million people (Chakraborti, *et al.,* 2017). Without taste, odor and color, As-polluted water is hardly detected and avoided from being exposed by local

✉ *Corresponding Author Email: teborano12@gmail.com*
Tel.: +66063 4678 119   Fax: +6604422 3053

people, and this makes it a main pathway to enter the human body (Sharma, *et al.,* 2014). A long-term ingestion of arsenic contaminated water can develop arsenicosis and other diseases such as cancers (bladder, kidney, lung, and skin), hypertensions, diabetes, respiratory disorders, neurological and liver issues (Jain and Singh, 2012; Yunus, *et al.,* 2011). In the environment, As can occur in oxidation states of -III, 0, III and V; however, trivalent [As(III)] or arsenite and pentavalent [As(V)] or arsenate are primarily found in natural water (Jain and Singh, 2012). Generally, a pretreatment is applied for converting As(III) to As(V) before elevated As-polluted water is treated to a safe or permissible level. However, the application of pretreatment has some drawbacks in term of time consuming, cost-addition and possibility of generating toxic by-products. Therefore, it is significant to use a proper removal technique that possibly remediate both As(III) and As(V). Several technologies used for the treatment include precipitation, ion exchange, coagulation, flocculation, reverse osmosis, membrane and adsorption. Compared to other methods, adsorption is more advantageous, suitable and promising because of the low cost, high adsorption efficiency and popularity in the developing world (Li, *et al.,* 2010). Either natural or synthetic materials such as commercial and synthetic activated carbons, agricultural product or by-products, industrial by-products or wastes, and metal oxides has been utilized as adsorbent (Mohan and Pittman, 2007). Currently, low-cost and effective adsorbents developed from natural materials supporting mental oxides or iron particles have widely been used to treat either As(III) or As(V) from water, i.e., As(V) adsorption onto adsorbents made from clay, iron oxide and starch (Chen, *et al.,* 2010); As(V) remediation by sand coated with zero-valent iron and iron oxide (Mak, *et al.,* 2011); As(III) and As(V) removal by montmorillonite-supported zero valent iron (Bhowmick, *et al.,* 2014); and As removal by iron mixed ceramic pellet (Shafiquzzam, *et al.,* 2013). However, the study of treating aqueous solutions with coexisting arsenate and arsenite [As(III+V)] is still limited. The main operational parameters affecting the adsorption efficiency in a batch experiment include contact time, adsorbent dosage, initial pH, and initial concentration. The interaction and optimization of those variables are normally investigated by a statistical technique like response surface methodology (RSM). RSM is considered as one of the most efficient statistical tools applied to design an experiment and simulate a model to evaluate the interactive influences of multiple factors and optimize the conditions (Roosta, *et al.,* 2014). The present study aims to use porous pellet adsorbent to investigate the optimization process of batch adsorption parameters for removing arsenate and arsenite coexisting in aqueous solutions. The main characteristics of the adsorbent were evaluated by various methods. Central composite design (CCD) under RSM was used as a main technique for this optimization process. The Pareto analysis was applied to obtain the variable effects on the adsorption efficiency in term of percentage. This study was carried out in environmental engineering laboratory at Suranaree University of Technology, Thailand in 2017.

MATERIALS AND METHODS
Development and characterization of adsorbent

Porous pellet adsorbent was developed by mixing natural clay, iron oxide, iron powder and rice bran. Natural clay (NC) with particle size of <75 μm was collected from Dankwian, Thailand. Iron oxide powder (Fe_2O_3, analytical grade, Himedia, India) was supplied by a chemical company. Iron powder (IP, industrial grade) and rice bran powder (RB) were purchased from a local supply store. The mixture was carried out at a ratio of 52.15% (NC):19.22% (Fe_2O_3):28.63% (IP), and 15% of RB was added for pore development. The detail procedure to define the optimal proportion is mentioned in another work (Te, *et al.,* 2017). The mixture was homogeneously mixed by adding deionized water slowly to produce a paste form. The paste was strongly stirred by hand for about 5-10min and dried at 104±1°C for 24 h, and further heated at 600°C for 2-3 h in a muffle furnace to carbonize the rice bran. After cooling down, the product was prepared for desired particle size of 0.6-1.12mm, and stored properly in a plastic container for further experiments. Brunauer-Emmett-Teller (BET) method was employed to determine surface area, total pore volume, and mean pore size of the adsorbent using N_2 adsorption-desorption isotherm data at 77 K (BELSORP Mini II, BEL Inc., Japan). Prior to the analysis, the adsorbent sample was outgassed under presence of N_2 at 60°C for 24 h. Surface morphological features were obtained from a scanning electron microscope (SEM, JSM-6010LV, JEOL, Japan). SEM

was coupled with Energy Dispersive X-ray to perform elemental composition analysis.

Adsorption experiments

The 200 mg/L stock solution [As(III) + As(V), 50% + 50%] was prepared from dissolving appropriate amount of $Na_2HAsO_4 \cdot 7H_2O$ and $NaAsO_2$ (Sigma Aldrich, USA) together into deionized (DI) water. Batch mode study was employed to conduct adsorption experiments at room temperature (25 ± 1°C) in 60 mL polyethylene bottles washed with acid and cleaned with DI water prior to being used. Mixtures of adsorbent and adsorbate were shaken on a horizontal mechanical shaker (New Brunswick Scientific, Canada) using 150 rpm agitation speed. Contact time, initial solution pH, adsorbent dosage and initial adsorbate concentration were varied from 24 to 72 h, 3 to 11, 0 to 20 g/L and 0.25 to 4.25 mg/L, respectively. Adjustment of solution pH was performed using either 0.1M HCl or NaOH. All samples were filtered through 0.45 μm syringe filters, acidified with 1%v/v HNO_3 and kept at 4°C till arsenic analysis within 24 h. Inductively Coupled Plasma-optical Emission Spectrometry (ICP-OES) (Optima 8000, PerkinElmer, USA) was used to measure the concentration of arsenic at the wavelength of 193.7 nm. The adsorption efficiency (A%) was calculated based on Eq. 1.

$$A\% = \frac{\left(C_i - C_f\right)}{C_i} \times 100 \tag{1}$$

Where, C_i and C_f (mg/L) are the initial and equilibrium concentration of adsorbate, respectively.

Experimental design and data analysis

The number of experiments (N) to be carried out for designing and analyzing the optimization process was obtained from Eq.2.

$$N = 2^k + 2k + n_c \tag{2}$$

Where, n_c and k are the number of central point replicates and independent variables, respectively. The adsorbate adsorption efficiency, as a response, is explained by the following model Eq.3.

$$Y = a_o + \sum_{i=1}^{q} a_i X_i + \sum_{i=1}^{q} a_{ii} X_{ii}^2 + \sum a_{ij} X_i X_j \tag{3}$$

Where, Y, X_i, and X_j represent the predicted responses, independent variables for factor *i*, and independent variables for factor *j*, respectively; a_0 and a_i are the constant and linear coefficients, respectively; a_{ii} and a_{ij} are the interactive and quadratic coefficients, respectively. The statistical and mathematical software (Minitab version 17.0, Minitab Inc., State College, PA) was used for designing the experiments, analyzing the data, fitting the models and optimizing the experimental conditions.

RESULTS AND DISCUSSION

Adsorbent characterization

Adsorption-desorption isotherm of N_2 from BET analysis and Barrett-Joyner-Halenda (BJH) pore size distribution for the adsorbent is depicted in Fig. 1.

According to the International Union of Pure and Applied Chemistry (IUPAC) classification, the
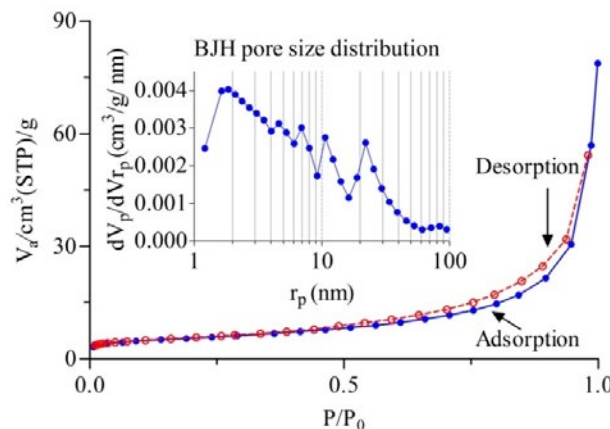
Fig. 1: Adsorption- desorption isotherm of N_2 for BET and BJH pore size distribution plots of the adsorbent

isotherm is a typical type IV and with the presence of hysteresis loop at high relative pressure, it demonstrates the mesoporous characteristic of the material. The graphical plot of BJH pore size distribution indicates that the material comprised of two main pore size ranges, the smaller mesopore of 2-10 nm and larger mesopore of 10-30 nm. Totally, the adsorbent significantly presents the pore size distribution between 2 nm and 50 nm, implying that it is a mesoporous adsorbent as defined by IUPAC classification for pore size ranges (Kuila and Prasad, 2013). From the BET analysis, the adsorbent exhibits 19.393 m^2/g, 0.0978 cm^3/g, and 20.169 nm for surface area, total pore volume, and mean pore size, respectively. Obtained from SEM analysis, Figs. 2a and 2b illustrate the adsorbent surface morphology before and after the adsorption, respectively. The adsorbent before the adsorption appears to have a rough surface structure with flat non-unified shape particles scattering around. After the adsorption

reaction, the surface of the adsorbent forms the concave morphology attached by spherical particles with various sizes. EDS analysis showed that the major elemental composition of the adsorbent was silica (Si_2O_4, 71.5%), alumina (Al_2O_3, 21.5%) and iron oxide (Fe_2O_3, 30.5%) (Fig. 2c). Several peaks of arsenic element were observed after the adsorption process (Fig. 2d).

Model development and analysis

The optimization process with CCD under RSM involves the following steps: defining the problem and the objective, identifying the factors or variables and their levels, designing the experimental matrix, conducting the designed experiments, performing the analysis and evaluation of the mathematical model, determining the optimal levels for variables, and conducting confirmation experiments (Massoudinejad, et al., 2016). In this work, independent variables are contact time (X_1), initial solution pH (X_2), adsorbent
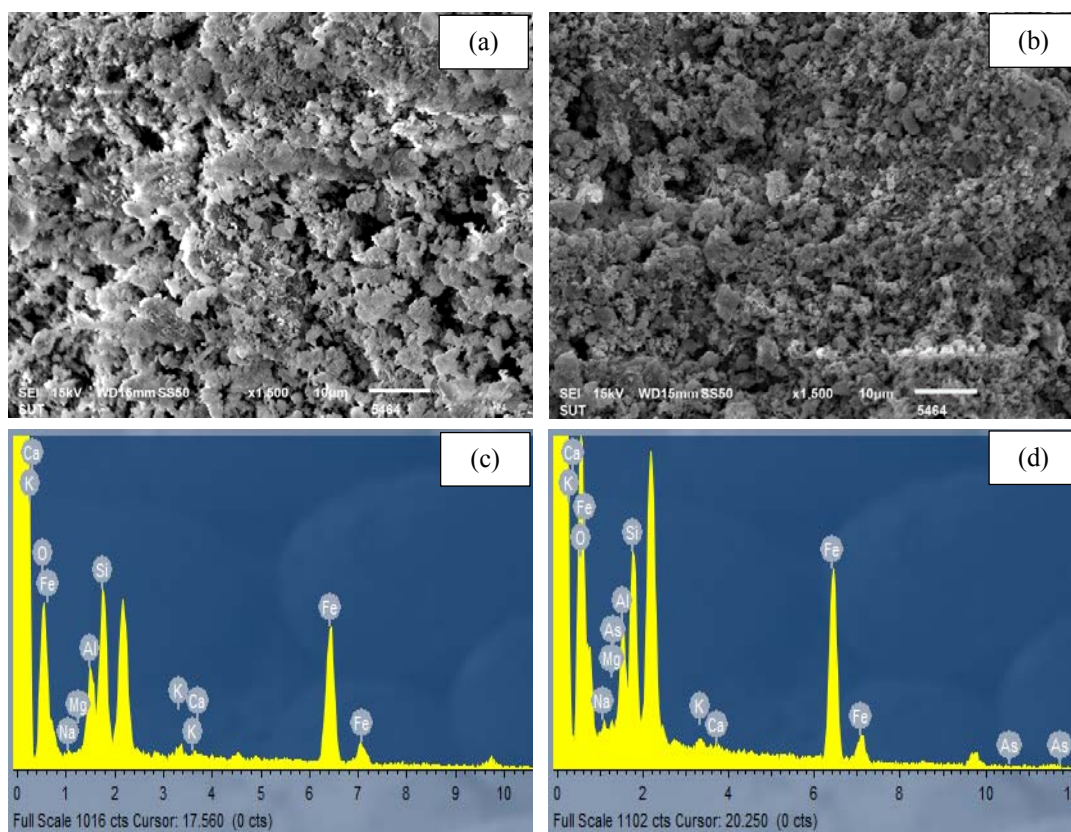
Fig. 2: SEM images of pre-adsorption of mesoporous pellet adsorbent (a), post-adsorption of mesoporous pellet adsorbent (b), and EDS analysis of the adsorbent before and after adsorption (c) and (d), respectively

Table 1: Experimental levels and representative codes of independent variables

Parameters	Codes	Level				
		$-\alpha$	-1	0	$+1$	$+\alpha$
Contact time (h)	X_1	24	36	48	60	72
Initial solution pH	X_2	3	5	7	9	11
Adsorbent dosage (g/L)	X_3	0	5	10	15	20
Initial adsorbate concentration (mg/L)	X_4	0.25	1.25	2.25	3.25	4.25

Table 2: A number of experimental run along with design points and corresponsive obtained responses

Run	X_1 (h)	X_2	X_3 (g/L)	X_4 (mg/L)	A(%)	Predicted A(%)
1	36	9	5	1.25	34.704	32.263
2	60	5	15	1.25	99.830	103.56
3	48	7	10	2.25	90.393	90.394
4	48	7	10	2.25	90.382	90.394
5	60	5	5	3.25	70.394	68.298
6	36	9	5	3.25	30.069	26.094
7	48	7	10	2.25	90.408	90.394
8	60	9	15	3.25	87.897	89.554
9	60	5	5	1.25	80.472	77.855
10	72	7	10	2.25	99.623	99.027
11	36	5	5	1.25	62.480	60.585
12	48	11	10	2.25	32.206	33.301
13	48	7	10	2.25	90.367	90.394
14	36	9	15	3.25	78.416	81.610
15	36	5	15	3.25	94.182	96.184
16	48	7	10	2.25	90.372	90.394
17	48	7	10	0.25	99.368	100.07
18	60	9	15	1.25	83.908	85.043
19	60	5	15	3.25	99.724	102.75
20	48	7	20	2.25	99.332	90.676
21	48	7	10	4.25	93.966	93.081
22	48	3	10	2.25	76.079	74.815
23	48	7	10	2.25	90.258	90.394
24	48	7	0	2.25	0.0560	9.4530
25	36	5	15	1.25	97.389	98.940
26	36	5	5	3.25	49.646	49.089
27	48	7	10	2.25	90.393	90.394
28	60	9	5	1.25	53.166	50.915
29	60	9	5	3.25	47.669	46.686
30	36	9	15	1.25	77.197	79.038
31	24	7	10	2.25	73.402	73.812

dosage (X_3) and initial adsorbate concentration (X_4), and their lower and higher levels were selected accordingly (Table 1).

According to the design of CCD under RSM based on factors and their levels selected, a total number of 31 experiments (16 factorial points, 8 axial points (α = 2) and 7 replicates at the center point) was established for response surface modeling. The experiments were designed at different combinations of the factors (variables) to obtain certain values of the response (the adsorbate adsorption efficiency) for further analysis. Table 2 presents the experimental design matrix with the observed and predicted results for simultaneous adsorption of arsenate and arsenite.

Analyzing from the above experimental data, the established relationship between the adsorbate adsorption efficiency (Y) and independent parameters was expressed as the following empirical mathematical Eq. 4.

$$Y = -75.9 + 1.523\,X_1 + 22.31\,X_2 + 12.20\,X_3 - 19.67\,X_4 - 0.00690\,X_1X_1 - 2.271\,X_2X_2 - 0.4033\,X_3X_3 + 1.545\,X_4X_4 + 0.0144\,X_1X_2 - 0.0527\,X_1X_3 + 0.0404\,X_1X_4 + 0.2105\,X_2X_3 + 0.666\,X_2X_4 + 0.437\,X_3X_4 \qquad (4)$$

To ensure the reliability of this chosen mathematical model for an adequate approximation or a prediction to the real experiment data, it has been proved through observing some supportive parameters. A number of

Table 3: ANOVA table for response surface quadratic model

	DF	SS	AMS	F	P
Model	14	19048.8	1360.63	84.58	<0.001
X_1	1	955.3	955.32	59.38	<0.001
X_2	1	2580.0	2579.99	160.38	<0.001
X_3	1	9942.8	9942.81	618.05	<0.001
X_4	1	73.3	73.34	4.56	0.049
X_1X_1	1	27.1	27.09	1.68	0.213
X_2X_2	1	2350.3	2350.28	146.10	<0.001
X_3X_3	1	2962.3	2962.27	184.14	<0.001
X_4X_4	1	70.1	70.06	4.36	0.053
X_1X_2	1	1.9	1.91	0.12	0.735
X_1X_3	1	160.2	160.19	9.96	0.006
X_1X_4	1	3.8	3.77	0.23	0.635
X_2X_3	1	70.9	70.88	4.41	0.052
X_2X_4	1	28.4	28.36	1.76	0.203
X_3X_4	1	76.3	76.30	4.74	0.045
Residual	16	257.4	16.09		
Total	30	19306.2			

Note: DF = Degree of freedom; SS = Sum of squares; AMS = Adjusted mean square; F = F-value; P = P-value; $R^2 = 0.9867$, R^2-adj = 0.9750

statistical parameters such as the Fisher test (F-value), P-value, regression coefficient (R^2) and adjusted regression coefficient (R^2-adj) can be used to evaluate the model adequacy and the significance of its terms (Alidokht, *et al.,* 2011). The values of those statistical parameters were obtained from analysis of variance (ANOVA) (Table 3). A mathematical model is considered as a well predictive tool for the experiment results when the obtained F-value is greater than the tabulated F-value for a particular degree of freedom and significance level or P-value is less than 0.05 for the 95% confidence level.

The selected model is considered to be statistically significant or adequate for describing the experimental results because, at the confidence level of 95%, the obtained P-value (<0.001) for the model is lower than 0.05 and the associated F-value was 84.58 obviously greater than the calculated tabulated F-value ($F_{0.05, 14, 16}$ = 2.68). Nair *et al.* (2014) suggested that a model is suitable and has a good prediction efficiency if the value of R^2 is close to 1 and more comparable to the value of R^2-adj, and if R^2 and R^2-adj are largely different, a model may include statistically insignificant terms. From the ANOVA results, the values of R^2 and R^2-adj of the predicted model were 0.9867 and 0.9750, respectively, very close to 1 and comparable to each other. It implies that the model satisfactorily provides a goodness of fit to the experimental results, and from R^2 of 0.9867, it suggests that the obtained model could not well describe only 1.33% of the total variations of the obtained adsorbate adsorption efficiency. Fig. 3 represents a graphical plot of the correlation between
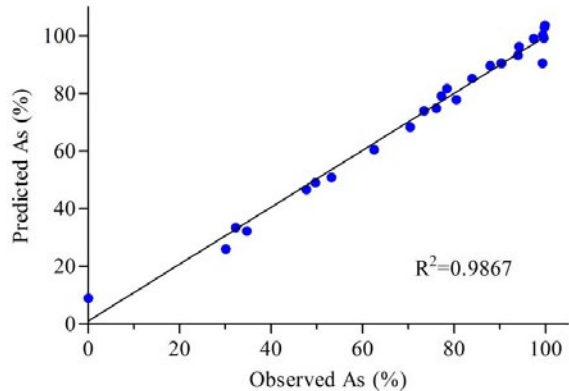
Fig. 3: Correlation of the predicted and actual results of the response

the predicted and actual values of the response.

The recorded measurement of the adsorbate adsorption efficiency (the response) in the real batch experiments provides the actual data set. The measure of the adsorption efficiency generated through the chosen mathematical model was the predicted data set. The agreement degree of the two data sets is evaluated in accordance with the value of the coefficient of determination obtained from a linear regression. The R^2 of the correlation between the predicted and actual data was found to be 0.9874, implying that the predicted values match the experimental values reasonably well. Graphical methods such as normal probability plot and the plot of residual versus fitted values were applied to observe the nature of residual data for evaluating the proportionality of the model.

The model with high proportionality should have a normal distribution of residual. For normal probability plot, the data is considered as a normal distribution when the obtained points stay close to the fitted straight line (Rostamiyan, *et al.,* 2014). As presented in Fig. 4a, the plotted points were apparently closer to the line, indicating the residual data normally distributed. On the other hand, the points in the plot of the residual versus fitted values scattered without obvious pattern, implying that the residuals were randomly distributed (Fig. 4b). Thus, the obtained empirical mathematical model is good enough to be used for the prediction.

The significance of each term of the model could be statistically checked using P-value. For the 95% confidence level, the term is statistically significant when its P-value is lower than 0.05. From the ANOVA analysis (Table 3), all individual terms (X_1, X_2, X_3, and X_4) ($p<0.05$) were significant to the response. For the quadratic or square terms, X_2X_2 and X_3X_3 were highly significant. The P-value of X_4X_4 was 0.053 (slightly greater than 0.05) implying very least insignificant and could be included in the model. For the interaction terms, X_1X_3 and X_3X_4 were significant for this response. It was also worth-noticing that X_2X_3 had P-value of 0.052, indicating less insignificant and possibly to be added. The developed model equation to be used as predictor for the response should be eliminated insignificant term. The individual or interactive effect of parameters on the adsorbate adsorption efficiency using the new developed adsorbent in term of the numerical percentage can be measured using the Pareto analysis. The analysis is possibly to identify factors that have the greatest cumulative effect or the least effect on the response. The calculation is in accordance with Eq. 5.

$$P_i = (b_i)^2/\sum(b_i)^2 \text{ x } 100 \quad (i{\neq}0) \qquad (5)$$

Where, P_i and b_i are the percentage effect and the parameter's related regression coefficient, respectively. The analysis results are illustrated in Fig. 5. It clearly indicated that among the designed factors, initial solution pH (47.69%), initial adsorbate concentration (37.07%), and adsorbent dosage (14.26%) provide the highest effect on the response.

Effect of variables

The three dimensional (3D) response surface and contour (2D) plots were developed based on the model equation in order to view interactive effects on the predicted response value by establishing various interactions of the investigated parameters. The plots were created by varying two variables within the designed range and keeping the other two constant. Figs. 6a and 6b represent the 3D surface plot and associating 2D contour plot for the response in term
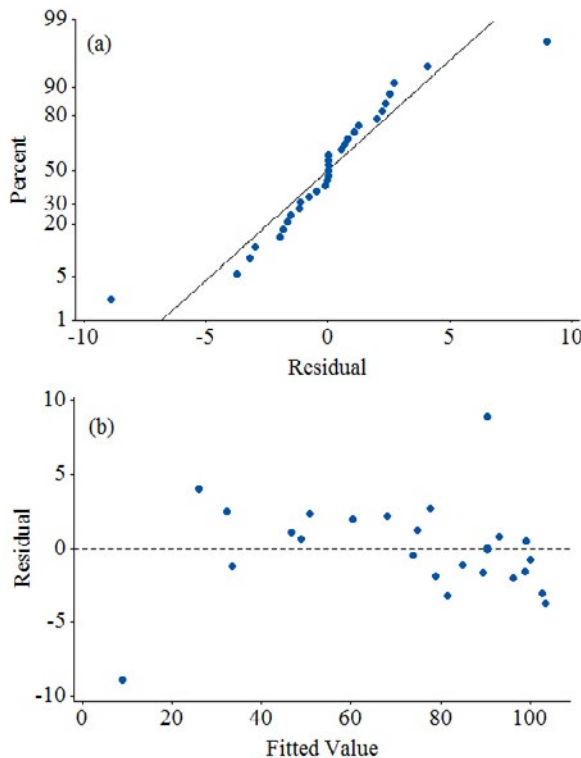
Fig. 4: Residual plots for the response: normality plot (a) and residual versus fitted result (b)
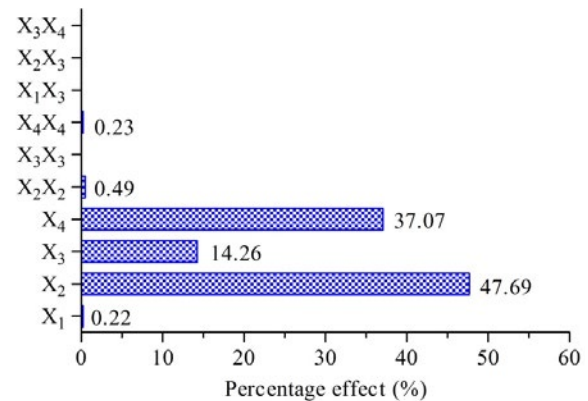
Fig. 5: Pareto graphic analysis for the percentage effect of the investigated factors

of the interaction effect of initial solution pH and initial concentration, respectively. Higher adsorption efficiency area represented by the darkest green color (> 95%) can be seen for the range pH of 3.5 to 7.5. The adsorption rate moved toward lower efficiency when increasing in pH values.

Solution pH significantly affects the adsorption of heavy metals due to its influence on speciation of metallic species, as well as the adsorbent surface charge (Prakash, *et al.,* 2008; Srivastava, *et al.,* 2015). In water, As(V) mainly exists in the form of H_3AsO_4 (pH <2.2), $H_2AsO_4^-$ (2.2< pH<6.98), $HAsO_4^{2-}$ (6.98<pH<11.5) and AsO_4^{3-} (pH>11.5) (Chang, *et al.,* 2010). As(III) species occur as: H_3AsO_3 (pH<9.2), $H_2AsO_3^-$ (9<pH<12), $HAsO_3^{2-}$ (12<pH<13), and AsO_3^{3-} (pH>13) (Mohan and Pittman, 2007). The surface of the adsorbent in this study is more positively charged for the acidic condition and predominated the negative charge for the alkaline pH (Te, *et al.,* 2017). This implied that the unfavorable electrostatic interaction or the electrical repulsion between the adsorbent and the adsorbate occurred for the high pH regions and resulted in low adsorption efficiency. Low adsorption efficiency region occurred when

the initial adsorbate concentration increased more than 1.5 mg/L. It could be due to an insufficiency of active sites on the adsorbent surface to adsorb more available adsorbate. Fig. 7a and 7b illustrate the plots of 3D surface and 2D contour, respectively, for the interactive effects of initial solution pH and adsorbent dosage on the response by constantly holding initial concentration and contact time. It can be clearly seen that increasing adsorbent dosage to above 10 g/L produced the highest removal percentage region within the range pH of 4 to 8. It occurred as expected because increasing in adsorbent dosage leads to having more available reactive sites for enhancing the adsorption between adsorbate and adsorbent. However, the adsorption efficiency became low when the amount of adsorbent is further increased. This is probably due to the reduction of effective surface area and adsorbate/adsorbent ratio (Ahma and Hasan, 2016).

The 3D and 2D plots of variation of adsorbate adsorption efficiency due to the influence of the combined effect of contact time and initial adsorbate concentration at a constant pH (7±0.1) and adsorbent dosage (10 g/L) is presented in Figs. 8a and 8b, respectively.
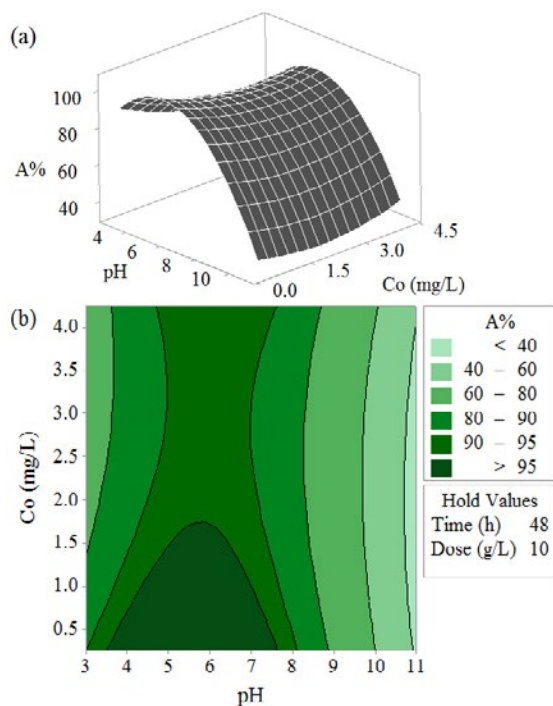
Fig. 6: Effect of initial solution pH and adsorbate concentration on the removal efficiency: (a) 3D response surface and (b) 2D contour plots
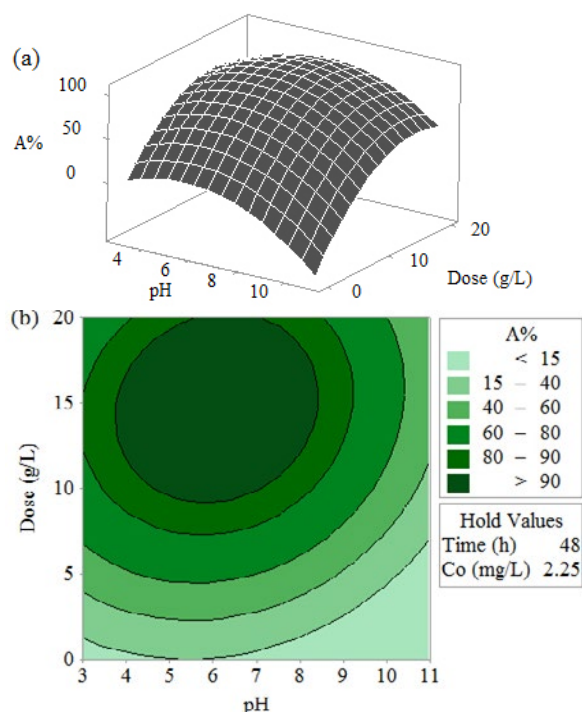
Fig. 7: Effect of initial solution pH and adsorbent dosage on the removal efficiency: (a) 3D response surface and (b) 2D contour plots
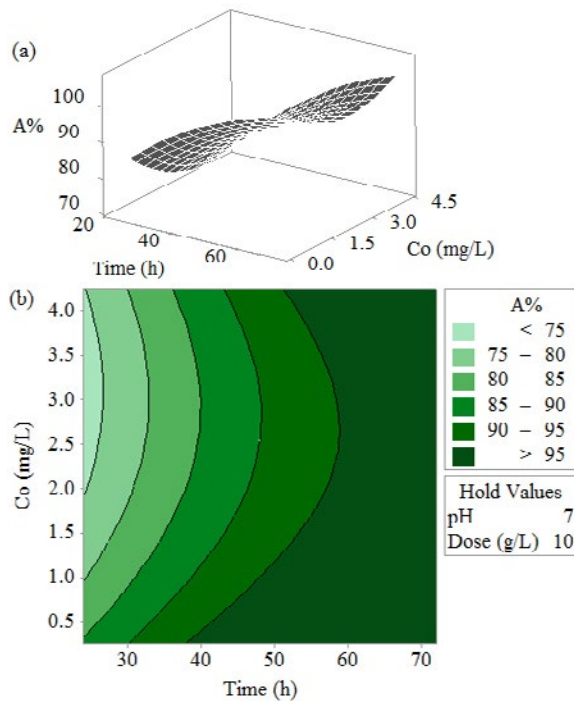
Fig. 8: Effect of contact time and initial adsorbate concentration on the removal efficiency: (a) 3D response surface and (b) 2D contour plots

From Fig. 8b, the removal efficiency increased with increasing in reaction time. Longer contact time means that it ensures to have enough amount of time for facilitating the interaction of adsorbate and adsorbent in the adsorption process. It is also observed that the reaction time to achieve the maximum adsorption rate took longer as the initial adsorbate concentration increased. This is probably due to the increase of adsorbate/adsorption sites. At higher initial concentration, it has more available adsorbate ions to fill on the limited number of adsorption site which leads to increasing time for adsorbing. On the other hand, Alidokht *et al.* (2011) suggested that a much more presence of adsorbate ions may result in losing reactivity on the surface of adsorbent due to a creation of the passivation.

Optimization and its validation

Response optimization involves defining independent variable settings that collaboratively produce the optimized arsenic adsorption efficiency, and its satisfactory is measured by the composite desirability (Rao and Baral, 2011). The desirability is scaled from 0.0 (undesirable) to 1.0 (very desirable). In this work, the process optimization was evaluated by Response Optimizer of Minitab. Fig. 9 shows the optimization plot of independent variables that affected the predicted adsorption efficiency. Independent variable settings on the plot could be adjusted by moving the vertical red line to obtain more desirable predicted responses. The result suggested that the ideal condition to achieve the most desirable adsorption efficiency of 99.9321% was contact time (52 h), initial solution pH (7), adsorbent dosage (10g/L) and initial adsorbate concentration (0.5mg/L). The predicted desirability (d and D) was found to be 1, implying that the selected optimized condition is suitable for producing the maximum As(V+III) adsorption efficiency.
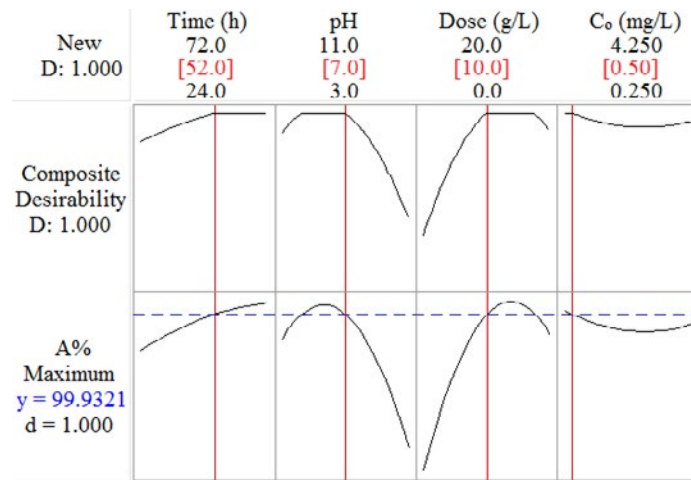
Fig. 9: Response optimization plot for the adsorbate adsorption efficiency

The optimum condition has been applied in the batch experiment for removing coexisting arsenate and arsenite aqueous solution by the mesoporous pellet adsorbent to validate the model. The results indicated that the removal efficiency was 99.8%, comparable enough to the predicted value. It suggests that the process optimization on removing coexisting arsenate and arsenite from water using the new developed mesoporous adsorbent was valid and adequate in the range of investigated parameters.

CONCLUSION

The new developed mesoporous pellet adsorbent has been used to adsorb coexisting arsenate and arsenite from aqueous solutions through batch experiments. The composite central design under response surface method was proved to be an easy scientific tool to study the optimization process for obtaining the most desirable adsorbate adsorption efficiency. The ANOVA analysis suggested the second polynomial mathematical model should be used and its adequacy was supported by F-value, P-value, R^2 and R^2-adj. The residual data was confirmed to have a normal distribution by the residual and normality plots. Initial solution pH, adsorbent dosage and initial adsorbate concentration provided the most percentage effect on the response. The optimum values of contact time, initial solution pH, adsorbent dosage and initial adsorbate concentration were 52 h, 7, 10 g/L and 0.5 mg/L, respectively. The confirmatory experiment was in agreement with the predicted model. The present study is simple, time saving and cost-effective to provide one specific optimum condition to remove highly toxic and carcinogenic pollutant by the adsorbent produced from low cost and widely availability of raw materials.

ACKNOWLEDGMENT

CONFLICT OF INTEREST

The author declares that there is no conflict of interests regarding the publication of this manuscript.

ABBREVIATIONS

$-\alpha$	Independent variable lower level
$+\alpha$	Independent variable higher level
$\mu g/L$	Microgram per liter
Al_2O_3	Alumina
AMS	Adjusted mean square
ANOVA	Analysis of variance
As(III + V)	Coexisting arsenate and arsenite
As(III)	Arsenite
As(V)	Arsenate
BET	Brunauer-Emmett-Teller method
BJH	Barrett-Joyner-Halenda
CCD	Central composite design
cm^3/g	Cubic centimeter per gram
DF	Degree of freedom
DI	Deionized
EDS	Energy dispersive X-ray
F	F-value
Fe_2O_3	Iron oxide
g/L	Gram per liter
h	Hour
HCl	Hydrochloric acid
HNO_3	Nitric acid
IARC	International Agency for Research on Cancer
ICP-OES	Inductively coupled plasma-optical emission spectrometry
IP	Iron powder
IUPAC	International union of pure and applied chemistry
m^2/g	Square meter per gram
mg/L	Milligram per liter
N_2	Nitrogen gas
$Na_2HAsO_4 \cdot 7H_2O$	Sodium hydrogen arsenate heptahydrate
$NaAsO_2$	Sodium arsenite
NaOH	Sodium hydroxide
NC	Natural clay
nm	Nanometer
P	P-value
pH	Potential of hydrogen
RB	Rice bran powder

RSM	Response surface methodology
SEM	Scanning electron microscope
Si_2O_4	Silica
SS	Sum of squares
$USEPA$	United State Environmental Protection Agency
v/v	Volume per volume
WHO	World Health Organization
X_1	Code for contact time (h)
X_2	Code for initial solution pH
X_3	Code for adsorbent dosage (g/L)
X_4	Code for initial adsorbate concentration (mg/L)

REFERENCES

Ahma, R.; Hasan, I., (2016). Optimiztion of the adsorption of Pb(II) from aqueous solution onto PAB nanocomposite using response surface methodology. Enivron. Nano. Monit. and Manag., 6(2016): 116-129 (**14 pages**).

Alidokht, L.; Khataee, A.R.; Reyhanitaba, A.; Oustan, S., (2011). Cr(VI) immobilization process in a Cr-spiked soil by zerovalent iron nanoparticle: Optimzation using response surface methodology. Clean- Soil, Air, Water, 39(7): 633-640 (**8 pages**).

Bhatia, S.; Balamurugan, G.; Baranwal, A., (2014). High arsenic contamination in drinking water hand-pumps in Khap Tola, West Champaran, Bihar, India. Front. Environ. Sci., 2(49):1-8 (**9 pages**).

Bhowmick, S.; Chakraborty, S.; Mondal, P.; Van Renterghem, W.; Van den Berghe, S.; Roman-Ross, G.; Chatterjee, D.; Iglesias, M., (2014). Montmorillonite-supported nanoscale zero-valent iron for removal of arsenic from aqueous solution: Kinetics and mechanism. Chem. Eng. J., 243(2014): 14-23 (**10 pages**).

Chakraborti, D.; Das, B.; Rahman, M.M.; Nayak, B.; Pal, A.; Sengupta, M.K.; Ahamed, S.; Hossain, M.A.; Chowdhury, U.K.; Biswas, B.K.; Saha, K.C.; Dutta, R.N., (2017). Arsenic in groundwater of the Kolkata Municipal Corporation (KMC), India: Critical review and modes of mitigation. Chemosphere, 180:437-447 (**11 pages**).

Chang, Q.; Lin, W.; Ying, W.C., (2010). Preparation of iron-impregnated granular activated carbon for arsenic removal from drinking water. J. Hazard. Mater., 184(1): 515-522 (**8 pages**).

Chen, R.; Zhang, Z.; Feng, C.; Hu, K.; Li, M.; Li, Y.; Shimizu, K.; Chen, N.; Sugiura, N., (2010). Application of simplex-centroid mixture design in developing and optimizing ceramic adsorbent for As(V) removal from water solution. Micro. Meso. Mater., 131(1): 115-121 (**7 pages**).

Habuda-Stanic, M.; Nujic, M., (2015). Arsenic removal by nanoparticles: a review. Environ. Sci. Pollu. Res., 22(11): 8094-8123 (**30 pages**).

Jain, C.K.; Singh, R.D., (2012). Technological options for the removal of arsenic with special reference to South East Asia. J. Env. Manage., 107(2012): 1-18 (**18 pages**).

Kuila, U.; Prasad, M., (2013). Specific surface area and pore-size distribution in clays and shales. Geophysical Prospecting, 61(2): 341-362 (**22 pages**).

Li, Y.; Wang, J.; Luan, Z.; Liang, Z., (2010). Arsenic removal from aqueous solution using ferrous based red mud sludge. J. Hazar. Mater., 177(1): 131-137 (**7 pages**).

Mak, M.S.; Rao, P.; Lo, I.M., (2011). Zero-valent iron and iron oxide-coated sand as a combination for removal of co-present chromate and arsenate from groundwater with humic acid. Environ. Pollu., 159(2): 377-382 (**6 pages**).

Massoudinejad, M.; Ghaderpoori, M.; Shahsavani, A.; Amini, M.M., (2016). Adsorption of fluoride over a metal organic framework Uio-66 functionalized with amine groups and optimization with response surface methodology. J. Molecu. Liqu., 221: 279-286 (**8 pages**).

Mohan, D.; Pittman, Jr.C.U., (2007). Arsenic removal from water/wastewater using adsorbents--A critical review. J. Hazar. Mater., 142(1): 1-53 (**53 pages**).

Nair, A.T.; Makwana, A.R.; Ahammed, M.M., (2014). The use of response surface methodology for modelling and analysis of water and wastewater treatment process: a review. Water Sci. Tech., 69(3): 464-478 (**15 pages**).

Prakash, O.; Talat, M.; Hasan, S.H.; Pandey, R.K., (2008). Factorial design for the optimization of enzymatic detection of cadmium in aqueous solution using immobilized urease from vegetable waste. Bioresour. Tech., 99(16): 7565-7572 (**8 pages**).

Rao, P.V.; Baral, S.S., (2011). Experimental design of mixture for the anaerobic co-digestion of sewage sludge. Chem. Eng. J., 172(2): 977-986 (**10 pages**).

Roosta, M.; Ghaedi, M.; Daneshfar, A.; Sahraei, R., (2014). Experimental design based response surface methodology optimization of ultrasonic assisted adsorption of safaranin O by tin sulfide nanoparticle loaded on activated carbon. Spectr. Acta Part A: Mole. Bio. Spect., 122(2014): 223-231 (**9 pages**).

Rostamiyan, Y.; Hamed, M.A.; SalmanKhani, A., (2014). Optimization of mechanical properties of epoxy-based hybrid nanocomposite: Effect of using nano silica and high-impact polystyrene by mixture design approach. Mater. Desig., 56(2014): 1068-1077 (**10 pages**).

Shafiquzzam, M.; Hasan, M.M.; Nakajima, J., (2013). Iron mixed ceramic pellet for arsenic removal from groundwater. Environ. Eng. Res., 18(3): 163-168 (**6 pages**).

Sharma, A.K.; Tjell, J.C.; Sloth, J.J.; Holm, P.E., (2014). Review of arsenic contamination, exposure through water and food and low cost mitigation options for rural areas. Appli. Geo., 41(2014): 11-33 (**24 pages**).

Srivastava, V.; Sharma, Y.C.; Sillanpaa, M., (2015). Response surface methodological approach for the optimization of adsorption process in the removal of Cr(VI) ions by $Cu_2(OH)_2CO_3$ nanoparticles. Appli. Sur. Sci., 326(2015): 257-270 (**14 pages**).

Te, B.; Wichitsathian, B.; Yossapol, C.; Wonglertarak, W., (2017). Development of low-cost iron mixed porous pellet adsorbent by mixture design approach and its application for arsenate and arsenite adsorption from water. Adsorp. Sci. Tech., 0-21 (**21 pages**).

Villaescusa, I.; Bollinger, J.-C., (2008). Arsenic in drinking water: sources, occurrence and health effects (a review). Rev. Env. Sci. Bio/Tech., 7(4): 307-323 (**17 pages**).

Yunus, M.; Sohel, N.; Hore, S.K.; Rahman, M., (2011). Arsenic exposure and adverse health effects: a review of recent findings from arsenic and health studies in Matlab, Bangladesh. Kaohsiung J. Medic. Sci., 27(9): 371-376 (**6 pages**).

AUTHOR (S) BIOSKETCHES

Te, B., Ph.D. Candidate, School of Environmental Engineering, Institute of Engineering, Suranaree University of Technology, Nakhon Ratchasima 30000, Thailand. Email: *teborano12@gmail.com*

Wichitsathian, B., Ph.D., Assistant Professor, Candidate, School of Environmental Engineering, Institute of Engineering, Suranaree University of Technology, Nakhon Ratchasima 30000, Thailand. Email: *boonchai@sut.ac.th*

Yossapol, C., Ph.D., School of Environmental Engineering, Institute of Engineering, Suranaree University of Technology, Nakhon Ratchasima 30000, Thailand. Email: *chatpet@sut.ac.th*

Wonglertarak, W., Ph.D. Candidate, School of Environmental Engineering, Institute of Engineering, Suranaree University of Technology, Nakhon Ratchasima 30000, Thailand. Email: *w_watcharapol@hotmail.com*